# Accurate and Efficient BER Calculation by Statistical Simulation Based on Physical Transmit Jitter Model

Fangyi Rao
Analog/RF and SI Simulation SW Expert
Agilent Technologies, EEsof-EDA
Santa Clara, CA
fangyi_rao@agilent.com

Sanjeev Gupta
Signal Integrity Applications Specialist
Agilent Technologies, EEsof-EDA
Santa Rosa, CA
sanjeev_gupta@agilent.com

***Abstract***

*Statistical analysis provides an efficient alternative to the traditional Monte Carlo simulation for extremely low BER calculation in high speed serial link designs. Transmitter (TX) jitter posts a huge challenge in statistical simulation due to its pattern- and time-dependent nature and the resulting computational complexity. This paper presents a fast yet rigorous approach to calculate TX jitter in statistical simulation based on physical models of various jitter components. The approach accurately captures effects of uncorrelated random jitters, jitter amplification by channel dispersion, frequency dependency of periodic jitter and data duty-cycle-distortion.*

*Keywords—serial link, statistical simulation, BER, jitter.*

## I. Introduction

As data rates in serial link systems advance, the nature of channel behavior becomes increasingly stochastic under the influence of various sources of jitter. As a result, statistical performance measurements, including bathtub curves and BER contours, become critical in channel design and verification. Since many applications specify eye openings at very low BER (e.g., 1e-12), where brute-force Monte-Carlo (MC) simulation isn't practical, methods such as StatEye have been developed to directly compute eye probability density functions (PDFs) by statistical calculations [1,2]. Statistical methods are efficient in calculating eye properties to extremely low BERs and have been widely adopted by the signal integrity community.

Because of its importance to high-speed serial link performance, accurate modeling of transmitter (TX) jitter and its various components -- including random jitter (RJ), periodic jitter (PJ) and duty-cycle-distortion (DCD) – is required in statistical channel simulations. To model the TX jitter contribution to the PDF at the channel output, StatEye-like methods use a formula of the form:

$$p(v,t) = \int p_{ISI}(v,t-\tau) \cdot p_{jitter}(\tau) d\tau \qquad (1)$$

where $p_{ISI}(v,t)$ is the channel ISI PDF and $p_{jitter}(t)$ is the TX jitter distribution. As the paper will show, this formula relies on simplified assumptions about TX jitter that lead to optimistic performance predictions [3]. In particular, they are valid only at the uniform jitter limit and fail to model effects of the high frequency behavior of PJ, RJ and DCD, and phenomena such as jitter amplification by the channel.

The recursive algorithm for fast ISI evaluation described in [1] is the key to efficient simulations that have made StatEye-based methods popular and de-facto standard for statistical channel analysis. The ideal transition time assumption that makes recursive ISI evaluation possible, as the paper will demonstrate, is violated by the presence of TX jitter. As a result, rigorous jitter modeling poses non-trivial challenges both in theory and in practical applications to highly efficient channel simulations.

Drawing upon the principles laid out in [3,4], this paper offers a new approach to statistical simulations that is both rigorous in its treatment of TX jitter – and therefore accurate – and efficient in practical EDA simulations. We demonstrate TX jitter's inherent time and pattern dependent nature and discuss its impact on numerical complexity and simulation performance. By including a rigorous, time- and pattern-dependent TX jitter model, our method is shown to accurately capture important effects that include: asymmetric rise and fall edges due to DCD; PJ frequency dependence; the effects of uncorrelated RJ sequence; jitter amplification by the channel; and cross-talk and equalization effects. The numerical complexity introduced by TX jitter is tackled by an advanced, NP-complete simulation algorithm.

To verify the accuracy of our approach, statistical simulation results are extensively compared to reference results obtained from a brute-force Monte Carlo method using long bit sequences, under various TX jitter conditions described by our TX jitter model. Excellent agreement is observed between the two methods. The proposed method is applied to serial link simulations with Algorithm Model Interface (AMI) SERDES models. We also investigate simulation results obtained from a StatEye-like approach using Equation (1) and explain their discrepancy with reference data.

## II. Physical Model of Transimit Jitter

A general TX jitter model is illustrated in Figure 1. It assumes uncorrelated RJ between different rise and fall edges, represents PJ with a sinusoidal function of time, and includes

DCD caused by asymmetric rising and falling data edges. The rise time $t_r$ and the fall time $t_f$ of the $i^{th}$ TX pulse are modulated by jitter functions $\tau_r$ and $\tau_f$ as:

$$\begin{aligned} t_r(i) &= n_r(i)\cdot T + \tau_r(i) \\ t_f(i) &= n_f(i)\cdot T + \tau_f(i) \end{aligned} \quad (2)$$

where $n_r$ is the bit index of the first 1-bit of the pulse, and $n_f$ is the index of the first 0-bit that follows it. $T$ is the unit interval and $n_r T$ and $n_f T$ represent ideal rise and fall times. In terms of RJ, PJ and DCD contributions,

$$\begin{aligned} \tau_r(i) &= \eta_r(i) + A\cos[\omega\cdot n_r(i)T + \phi] - \frac{\Delta}{2} \\ \tau_f(i) &= \eta_f(i) + A\cos[\omega\cdot n_f(i)T + \phi] + \frac{\Delta}{2} \end{aligned} \quad (3)$$

where $\eta_r$ and $\eta_f$ represent random jitter at the rise and fall edges; $A$ and $\omega$ are the amplitude and frequency of the periodic jitter; and $\Delta$ terms model DCD due to asymmetry between the rising and falling edges, with opposite signs for $\tau_r$ and $\tau_f$.

Equations (2) and (3) reveal several important characteristics of TX jitter. First, as shown in Figure 1, jitter occurs only at physical rise and fall edges; in pulses with consecutive logic 1-bits only the first and the last bits are affected by jitter. Second, random jitters $\eta$ in Equation (3) are uncorrelated between different edges. Third, the DCD term alternates in sign between edges. As a result, all jitter components in the model are inherently time and bit pattern dependent. Importantly, RJ and DCD vary with time at rates comparable to the data rate and thus contain significant high frequency spectrum content.

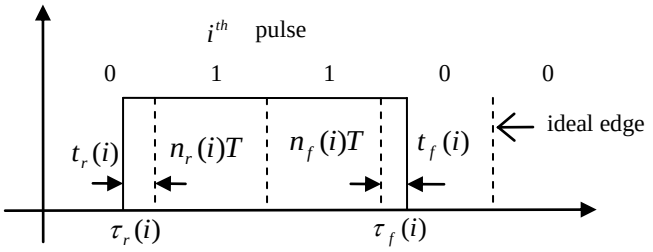


Figure 1: TX jitter model. Solid vertical lines represent the actual rising and falling edges. Dash lines represent ideal edges.

Given a channel impulse response length *M*, measured in bits, a sample time *t*, and the expected logic level at the channel output, the number of possible random bit patterns that contribute to the output voltage $v(t)$ is $2^M - 1$. For the $m^{th}$ pattern, the channel output $v^{(m)}$ can be calculated by the superposition of the rising step response R(t) and the falling step response F(t) of the channel as:

$$v^{(m)}(t) = \sum_i \left\{R[t - t_r^{(m)}(i)] - F[t - t_f^{(m)}(i)]\right\} + v_0 \quad (4)$$

where $t_r^{(m)}(i)$ and $t_f^{(m)}(i)$ are rise and fall times of the $i^{th}$ pulse in the $m^{th}$ pattern, and $v_0$ is the output when all input bits are logic 0. Equation (4) shows that TX jitter and channel ISI are interdependent and cannot be treated separately in general. Statistical calculations based on rigorous TX jitter models must take into account jitter at all pulse edges in all patterns. Enormous computational complexity is introduced to statistical simulations by jitter dependencies on time and bit pattern.

When TX jitter is zero, only ISI is responsible for the output jitter and Equation (4) becomes

$$v_{ISI}^{(m)}(t) = \sum_i \left\{R[t - n_r^{(m)}(i)\cdot T] - F[t - n_f^{(m)}(i)\cdot T]\right\} + v_0 \quad (5)$$

where $n_r^{(m)}(i)$ is the bit index of the first 1 bit of the $i^{th}$ pulse in the $m^{th}$ pattern and $n_f^{(m)}(i)$ is the bit index of the first 0 bit follows that pulse. The ISI PDF $p_{ISI}$ of the expected logic level at time *t*, as a function of output voltage, is given by the distribution of $v^{(m)}$ for all $2^M - 1$ patterns.

$$p_{ISI}(v,t) = \frac{1}{2^M - 1}\sum_m \delta[v - v_{ISI}^{(m)}(t)] \quad (6)$$

where $\delta$ is the Dirac delta function. When rise and fall edges are symmetrical, functions R and F are the same and Equation (6) can be evaluated efficiently by recursive PDF convolution based on the ideal single bit pulse response given by R(t)-R(t+T) [1,2].

StatEye-like TX jitter treatment, shown in Equation (1), follows from Equation (4) in the special case where TX jitter is assumed to be constant. In that case, all $\tau_r$ and $\tau_f$ in Equation (2) have the same value $\tau$, Equation (4) further simplifies to:

$$\begin{aligned} v^{(m)}(t,\tau) &= \sum_i \left\{R[t - n_r^{(m)}(i)\cdot T - \tau] - F[t - n_f^{(m)}(i)\cdot T - \tau]\right\} + v_0 \\ &= v_{ISI}^{(m)}(t - \tau) \end{aligned} \quad (7)$$

The PDF of the expected logic level at the output is given by

$$p(v,t) = \frac{1}{2^M - 1}\sum_m \int \delta[v - v^{(m)}(t,\tau)]\cdot p_{jitter}(\tau)\,d\tau \quad (8)$$

where $p_{jitter}$ is the TX jitter distribution. Combining Equations (6) - (8), we arrive at the StatEye jitter model in Equation (1):

$$p(v,t) = \int p_{ISI}(v, t-\tau) \cdot p_{jitter}(\tau) d\tau \quad (9)$$

This analysis demonstrates that TX jitter modeling by Equation (1) applies only if jitter is independent of time/edge, or varies slowly within the length of the channel impulse response. These conditions do not hold in practice where, as argued earlier, both DCD and uncorrelated RJ carry high frequency components and PJ can vary significantly over impulse length.

## III. Jitter Amplification by Channel

Jitter amplification by the channel is a phenomenon arising from interactions between TX jitter and channel ISI [5,6]. This effect is predicted by the rigorous TX jitter model in Equation (4).

Consider the output crossing time as given by Equation (4):

$$\begin{aligned} v_{th} = \sum_i \{ & R[t_c^{(m)} + \delta t_m - n_r^{(m)}(i)T + \frac{\Delta}{2} - \eta_r^{(m)}(i)] \\ & - F[t_c^{(m)} + \delta t_m - n_f^{(m)}(i)T - \frac{\Delta}{2} - \eta_f^{(m)}(i)]\} + v_0 \end{aligned} \quad (10)$$

where $v_{th}$ is the crossing threshold, $t_c^{(m)}$ is the zero-RJ crossing time for the $m^{th}$ pattern, and $\delta t_m$ the shift in crossing time induced by RJ $\eta_r^{(m)}$ and $\eta_f^{(m)}$. PJ is set to zero to simplify discussion.

Under the condition of small RJ, $\delta t^{(m)}$ is given by linearization of Equation (10) around $t_c^{(m)}$:

$$\delta t_m = \frac{\sum_i \left[ R'_m(i) \cdot \eta_r^{(m)}(i) - F'_m(i) \cdot \eta_f^{(m)}(i) \right]}{\sum_i \left[ R'_m(i) - F'_m(i) \right]} \quad (11)$$

where

$$\begin{aligned} R'_m(i) &= \frac{dR[t_c^{(m)} - n_r^{(m)}(i) + \Delta/2]}{dt} \\ F'_m(i) &= \frac{dF[t_c^{(m)} - n_f^{(m)}(i) - \Delta/2]}{dt} \end{aligned} \quad (12)$$

Timing jitter at the output is characterized by the standard deviation $\sigma$ of the crossing time:

$$\sigma^2 = \frac{1}{2^M - 1} \sum_m \left\langle \left( t_c^{(m)} + \delta t_m \right)^2 \right\rangle - \bar{t}_c^{\,2} \quad (13)$$

where $\bar{t}_c$ is the averaged crossing time defined as

$$\bar{t}_c = \frac{1}{2^M - 1} \sum_m t_c^{(m)} \quad (14)$$

The average $\langle \cdots \rangle$ is taken over all $\eta_r^{(m)}$ and $\eta_f^{(m)}$. Equation (13) can be rewritten as

$$\begin{aligned} \sigma^2 &= \sigma_{DJ}^2 + \sigma_{RJ}^2 \\ \sigma_{DJ}^2 &= \frac{1}{2^M - 1} \sum_m t_c^{(m)\,2} - \bar{t}_c^{\,2} \\ \sigma_{RJ}^2 &= \frac{1}{2^M - 1} \sum_m \left\langle \delta t_m^{\,2} \right\rangle \end{aligned} \quad (15)$$

As shown in Equation (15), the output jitter consists of deterministic jitter $\sigma_{DJ}$ arising from ISI and DCD, and random jitter $\sigma_{RJ}$ induced by TX RJ. For uncorrelated TX RJ,

$$\begin{aligned} \sigma_{RJ}^2 &= \frac{1}{2^M - 1} \sum_m \frac{\sum_i R'_m(i)^2 \cdot \left\langle \eta_r^{(m)}(i)^2 \right\rangle + \sum_i F'_m(i)^2 \cdot \left\langle \eta_f^{(m)}(i)^2 \right\rangle}{\left\{ \sum_i \left[ R'_m(i) - F'_m(i) \right] \right\}^2} \\ &= \sigma_{TXRJ}^2 \frac{1}{2^M - 1} \sum_m \frac{\sum_i R'_m(i)^2 + \sum_i F'_m(i)^2}{\left\{ \sum_i \left[ R'_m(i) - F'_m(i) \right] \right\}^2} \end{aligned} \quad (16)$$

where $\sigma_{TXRJ}$ is the standard deviation of $\eta_r^{(m)}$ and $\eta_f^{(m)}$. Equation (16) shows that, due to ISI, output RJ comprises contributions from multiple TX edges. When RJs in these edges are uncorrelated, they contribute to the output independently and the effects are accumulated in the timing variance. When the factor following $\sigma_{TXRJ}$ in Equation (16) is great than one, TX RJ is amplified by the channel. As shown in the next section, practical channels can exhibit jitter amplification, especially at high data rates.

In the case of uniform TX RJ, $\eta_r^{(m)}$, $\eta_f^{(m)}$ and $\delta t_m$ are the same and $\sigma_{RJ} = \sigma_{TXRJ}$. Equation (15) becomes

$$\sigma^2 = \sigma_{DJ}^2 + \sigma_{TXRJ}^2 \quad (17)$$

Equation (17) also follows from Equation (1) at zero DCD, as a consequence of PDF convolution between ISI and TX RJ. Therefore, in StatEye-like calculations the output RJ is always equal to TX RJ. As a result, StatEye-like simulations fail to predict jitter amplification by the channel.

## IV. Rigorous Statistical Simulation with TX Jitter

To model TX jitter accurately and without approximation, the rigorous jitter model represented by Equations (2) and (3) is now applied to statistical simulation. The output PDF of the expected logic level is given by

$$p(v,t)=\frac{1}{2\pi}\int_0^{2\pi}d\phi\frac{1}{2^M-1}\sum_m\int\delta[v-v^{(m)}(t)] \cdot\prod_i g[\eta_r^{(m)}(i)]\cdot g[\eta_f^{(m)}(i)]\cdot d\eta_r^{(m)}(i)\cdot d\eta_f^{(m)}(i) \quad (18)$$

where $\eta_r^{(m)}(i)$ and $\eta_f^{(m)}(i)$ model random jitter at rising and falling edges of the $i^{th}$ pulse in the $m^{th}$ pattern, and $g(\eta)$ is the RJ PDF, typically a Gaussian distribution. The product of g functions in Equation (18) is the result of uncorrelated RJ at different edges. The channel output $v^{(m)}(t)$ is given by Equation (4). The PDF is averaged over the PJ phase offset, $\phi$, to account for its randomness relative to the data signal. As shown by Equation (18), our calculation includes TX RJ, PJ and DCD due to asymmetric rising and falling edges.

As discussed earlier, TX jitter is both time and pattern dependent and must be treated simultaneously with ISI. With the presence of TX jitter, pulse lengths are not ideal, so recursive PDF convolution based on the single bit pulse response for pure ISI is no longer applicable. For an impulse response *M* bits long, the numerical complexity of Equation (18) is $O(2^M)$, making a brute-force evaluation impractical.

To overcome the computational complexity introduced by TX jitter, an NP complete algorithm is developed to evaluate Equation (18) efficiently. The channel output PDF is computed rigorously and without approximation, such as step response linearization or low probability extrapolation, making it possible to accurately evaluate link performance to arbitrarily low BERs. The method has been extended to include the effects of crosstalk, equalization and receiver (RX) jitter.

Effects of crosstalk channels are taken into account as follows. When crosstalk is *synchronous*, aggressors are applied at the same data rate and at a fixed phase relationship to the main channel. When crosstalk is *asynchronous*, the aggressors' phase relationship varies relative to the main channel, either because their data rates are different or because the phase offset drifts. In the proposed method, crosstalk signals are treated as additive noise at the output. When the primary and aggressor transmitter bit sequences are mutually uncorrelated, the effects of crosstalk can be calculated by convolving the output PDFs of the primary and crosstalk signals along the voltage axis. For synchronous crosstalk,

$$p(v,t)=\int p_{main}(v-v_1-v_2\cdots-v_n,t) \cdot p_{xtlk}^{(1)}(v_1,t)p_{xtlk}^{(2)}(v_2,t)\cdots p_{xtlk}^{(n)}(v_n,t)dv_1dv_2\cdots dv_n \quad (19)$$

where $p_{main}$ and $p_{xtlk}^{(i)}$ are the PDFs of the main channel and the $i^{th}$ crosstalk channel calculated by Equation (18). For asynchronous crosstalk, in order to represent the random phase between the main and crosstalk channels, $p_{xtlk}^{(i)}$ is averaged along the time axis across one crosstalk UI, $T^{(i)}$. The averaged PDF is then convolved with $p_{main}$ at each time point as follows:

$$\bar{p}_{xtlk}^{(i)}(v)=\frac{1}{T^{(i)}}\int p_{xtlk}^{(i)}(v,t)dt$$
$$p(v,t)=\int p_{main}(v-v_1-v_2\cdots-v_n,t) \cdot\bar{p}_{xtlk}^{(1)}(v_1)\bar{p}_{xtlk}^{(2)}(v_2)\cdots\bar{p}_{xtlk}^{(n)}(v_n)dv_1dv_2\cdots dv_n \quad (20)$$

To model linear TX/RX equalization, continuous-time linear (CTLE) and feed-forward (FFE) equalizers are combined with the channel impulse response by standard convolution techniques. Under the approximation of zero decision error, decision feedback equalizers (DFE) are linear and are included in Equation (4) as:

$$v^{(m)}(t)=\sum_i\left\{R[t-t_r^{(m)}(i)]-F[t-t_f^{(m)}(i)]\right\} +\sum_k c_k\cdot b^{(m)}(t-kT)+v_0 \quad (21)$$

where $c_k$ is the $k^{th}$ DFE tap coefficient and $b^{(m)}(t)$ is the expected bit at the slicer output at time t in the $m^{th}$ bit pattern.

RX sampling time jitter effectively shifts the eye along the time axis. The averaged eye is calculated by convolving $p(v,t)$ with the RX jitter distribution.

## V. Simulation Results and Discussion

A Molex channel is simulated under different TX jitter conditions. The channel is represented by measured S-parameters as plotted in Figure 2. The same jitter model, described by Equations (2) and (3), is applied in both the proposed statistical approach and in Monte-Carlo (MC) simulations.

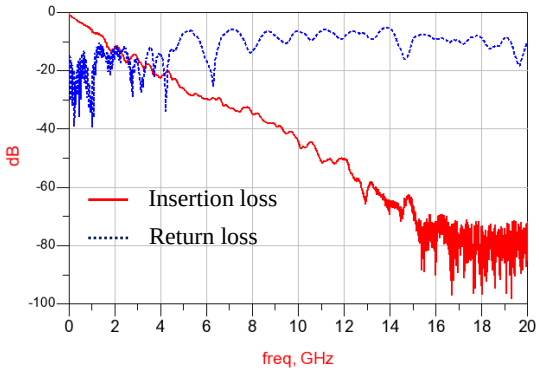


Figure 2: S-parameters of the main channel

### ISI Jitter

Figure 3 shows simulation results for 3 Gbps data rate with zero TX jitter, as calculated by the proposed statistical

approach. The output jitter is solely due to ISI. The ISI jitter RMS measured at the crossing level is 21.03ps.

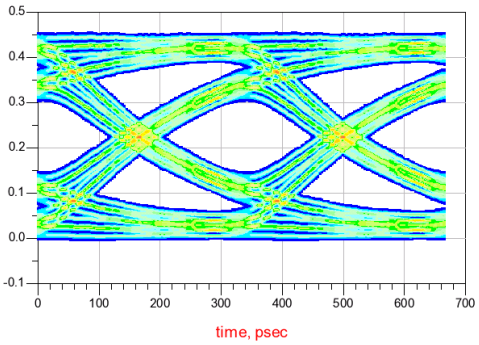


Figure 3: Eye diagram at 3 Gbps with zero TX jitter.

Table 1 lists the simulated worst-case eye width and height and compares them to Monte Carlo simulations with $10^3$ and $10^6$ bits. As expected, the longer the Monte Carlo run, the closer it converges to statistical analysis predictions.

| Method | 1K bits MC | 1M bits MC | Proposed method |
|---|---|---|---|
| width | 254ps | 244ps | 244ps |
| height | 0.164V | 0.157V | 0.155V |

Table 1: Width and height of the worst-case eye border at 3Gbps with zero TX jitter.

**TX Random Jitter**

In the next experiment, 5% UI (16.66ps) random jitter is applied to the TX. Eye diagrams and timing bathtub curves are displayed in Figures 4 and 5. Results of the proposed approach, utilizing Equations (2) and (3) to model jitter, are compared to a Monte Carlo simulation with one million bits and to a StatEye-based approach making use of Equation (1) for TX RJ. In the Monte Carlo simulation, where no sample data is available, the BER is set to zero (approximately below BER=1e-6).

The excellent agreement between the proposed statistical approach and the Monte Carlo simulation within the applicable range (BER above 1e-6) demonstrates the accuracy of the method presented in this paper. Note that, despite being induced by the same Gaussian TX RJ, the output random jitters on different sides of the crossing time are asymmetric as a consequence of pattern-dependence of TX jitter. Observe that the StatEye-based method overestimates the eye opening: whereas the rigorous approach predicts a closed eye at 1e-12 BER, calculations using Equation (1) predict a 41 ps wide opening.

Table 2 lists the total and random jitter components measured at the output. The random jitter is extracted from the total jitter according to Equation (15) and using 21.03 ps ISI jitter RMS reported in the earlier experiment. Results show that in the proposed method RJ is amplified by the channel from 16.66 ps at the input to 20.94 ps at the output. As shown earlier in the paper, the StatEye-based approach predicts no jitter amplification and underestimates random jitter at the output.

(a) Proposed method

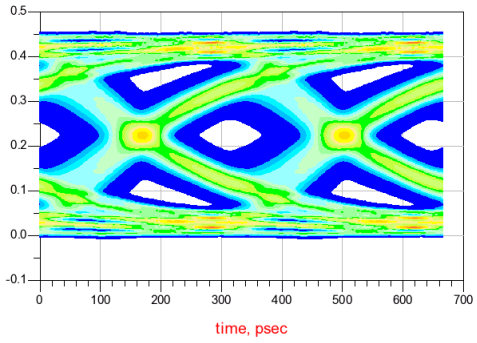


(b) 1M bits MC

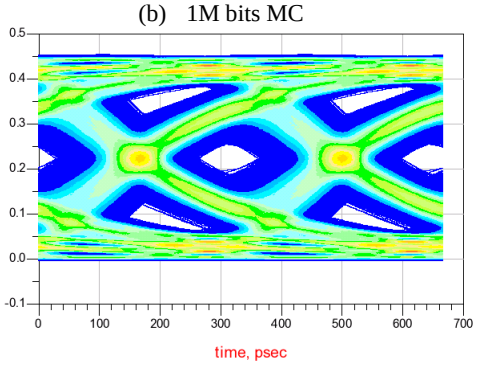


(c) StatEye-based

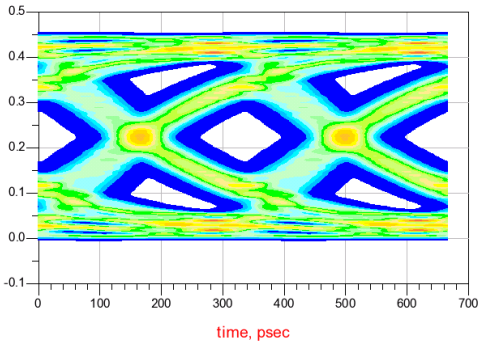


Figure 4: Eye diagrams at 3 Gbps with 5% UI TX random jitter.

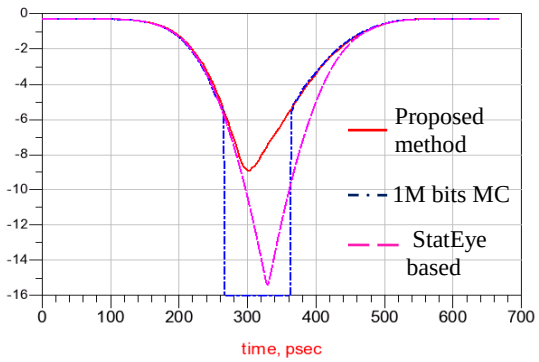


Figure 5: Timing bathtubs at 3 Gbps with 5% UI TX random jitter.

| Method | Total jitter RMS | RJ RMS |
|---|---|---|
| Proposed method | 29.68ps | 20.94ps |
| StatEye-based | 26.83ps | 16.66ps |

Table 2: Total and random RMS jitter at 3 Gbps with 5% UI TX random jitter. RJ RMS is extracted from total jitter according to Equation (15), using 21.03 ps ISI RMS jitter with TX RJ equal to zero.

Figure 6 shows the RJ amplification factor of the channel as a function of data rate calculated by the proposed method. Amplification factor is defined as the RMS ratio between RJ at the output and RJ at TX, which is fixed at 2%. As shown in the plot, the amplification effect increases with the data rate, suggesting it is caused by ISI, as predicted by theory.

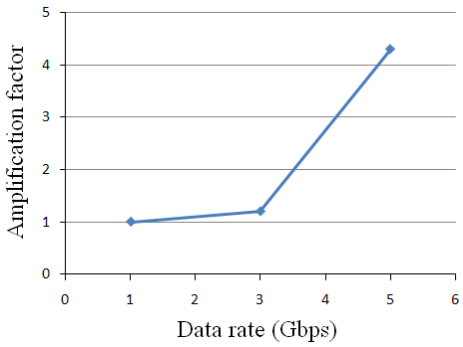


Figure 6: RJ amplification factor of the channel at different data rates.

The efficiency of the proposed method is highlighted in Table 3 by the CPU time comparison between statistical and Monte Carlo simulations (using $10^6$ bits) on a typical workstation.

| Method | Proposed method | 1M bits MC |
|---|---|---|
| CPU time | 7 sec | 198 sec |

Table 3: CPU times of the proposed statistical analysis and the Monte Carlo simulation of one million bits at 3 Gbps and 5% UI TX RJ.

### TX Periodic Jitter

In this experiment, we compare statistical and Monte Carlo simulations under TX periodic jitter with amplitude at 50 ps and different frequencies up to 500 MHz. The dependency of worst-case eye width on the PJ frequency is plotted in Figure 7. Due to limited sample size, Monte Carlo simulations always give a larger eye width than the proposed statistical method. Despite the difference, both methods predict decreasing eye open with increasing PJ frequency.

Figure 7 also includes the result obtained by a Stateye-based approach. In StatEye-based calculations, the PJ contribution is modeled by Equation (1) and the PJ distribution is given by:

$$p_{PJ}(x) = \frac{1}{\pi\sqrt{A^2 - x^2}} \qquad (22)$$

where x is the jitter and A is the PJ amplitude. Equation (22) does not depend on frequency and cannot account for the frequency-dependent effects. Note the StatEye result matches the proposed method at low frequency but differs at high frequency, confirming the expected failure of Equation (1) to model high-frequency jitter.

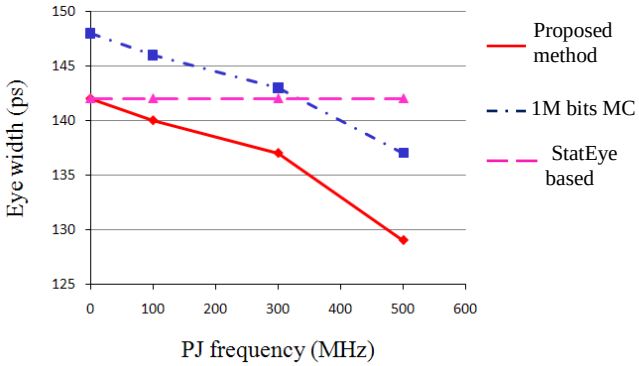


Figure 7: Worst-case eye width at 3 Gbps at different TX PJ frequencies.

### TX DCD

Figure 8 shows the eye diagram at 3 Gbps with 15% TX DCD calculated by the proposed method. Compared to Figure 3, the eye becomes asymmetric and the crossing level is shifted upward by 33 mV, indicating longer logic 1 cycles. As discussed in previous sections, Equation (2) models DCD caused by asymmetry between the rising and falling edges of the data signal, where all rising edges shift in one direction and all falling edges shift in the opposite direction. This type of DCD is manifested by a shift of crossing level toward the logic level with longer duration. Such a shift cannot be reproduced by Equation (1) because the convolution is performed along the time axis. Another type of DCD, caused by imbalance between the 1 and 0 bits of the clock signal, can also be treated by the proposed method with minor modifications.

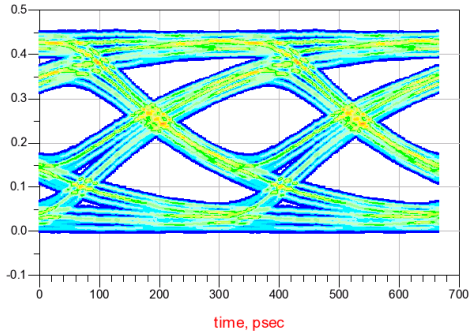


Figure 8: Eye diagram at 3Gbps with 15% TX DCD.

### Crosstalk

Synchronous near end (NEXT) and far end (FEXT) crosstalk are simulated with the proposed statistical method. The relative signal phase between the aggressor and the main channel is set to zero. S-parameters between aggressor and

receiver ports are plotted in Figure 9. Calculated eye diagrams are shown in Figure 10. As expected, the channel performance is impaired by both NEXT and FEXT compared to Figure 3, with more degradation caused by NEXT because of stronger coupling to the main channel.

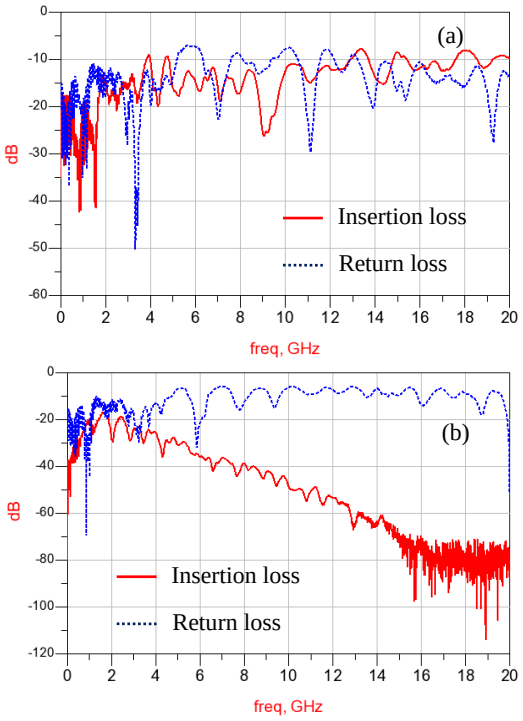


Figure 9: S-parameters between aggressor and receiver ports for (a) NEXT, and (b) FEXT.

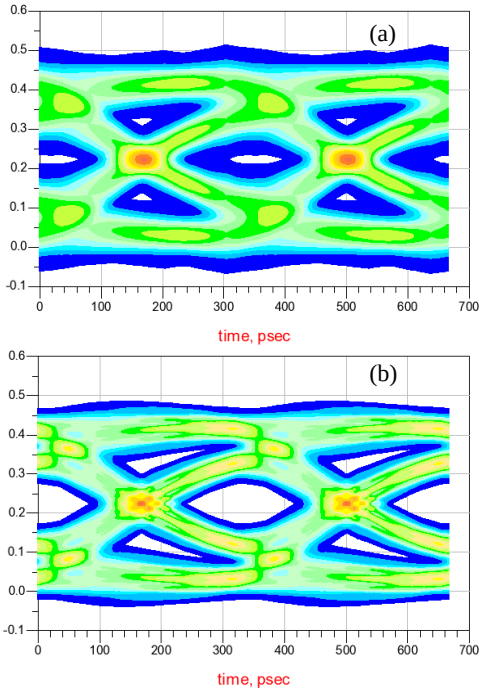


Figure 10: Eye diagrams at 3 Gbps with (a) NEXT, and (b) FEXT.

**Equalization**

A 6-tap (2 pre-cursors and 4 post-cursors) FFE and a 6-tap DFE are applied to the channel at 5 Gbps. Tap coefficients are optimized based on the channel impulse response. A 2% UI Gaussian jitter is used to model RX sampling jitter. Eye diagrams calculated by the proposed method are plotted in Figure 11. As shown in Figure 11, the eye is completely closed by ISI without equalization. It is opened by FFE and DFE.

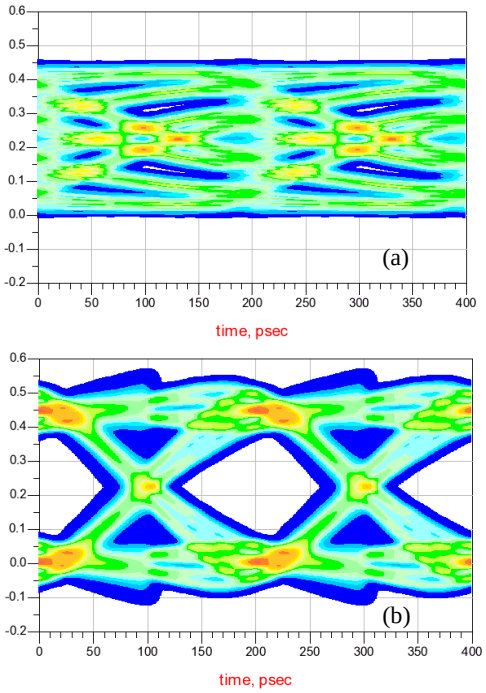


Figure 11: Eye diagrams at 5 Gbps (a) w/o, and (b) with equalization.

## VI. Appication to AMI Models

AMI (Algorithmic Modeling Interface) is a modeling interface for behavioral SERDES models defined in the IBIS standard [7]. The AMI simulation methodology divides the serial link into three blocks, namely the TX AMI block, the analog channel and the RX AMI block. The AMI block models operations happen inside the SERDES such as equalization and clock-data-recovery (CDR). It processes the input waveform and returns a modified waveform. The RX AMI block can also return clock ticks generated by CDR. The analog channel consists of the IBIS model of the TX backend, the physical channel and the IBIS model of the RX frontend. It's assumed that there is no electrical coupling between AMI blocks and the analog channel. It's also assumed that the channel is a linear time-invariant (LTI) system and can be represented by its impulse response. As a result, AMI simulation is greatly simplified compared to the traditional SPICE simulation and is capable to simulate millions of bits in minutes. Because of its speed advantage, the AMI

methodology is widely adopted in the high speed serial link industrial.

While AMI models are mostly used in time-domain bit-by-bit simulations as they model nonlinear behaviors of DFE and CDR, the AMI standard allows models to support statistical simulation by providing the impulse response representation of the SERDES under linear approximations. By combining impulse responses of AMI blocks and the channel, the approach presented in this paper can be applied to conduct statistical calculations on AMI models.

Figure 12 shows eye diagrams of the Molex channel with AMI TX and RX models at 3Gpbs calculated by the proposed statistical method and by a bit-by-bit simulation with one million bits. DFE effects are visible in both eye diagrams. The statistical result using the approximate impulse response returned by models is shown to be in qualitative agreement with the result of the more accurate time-domain simulation.

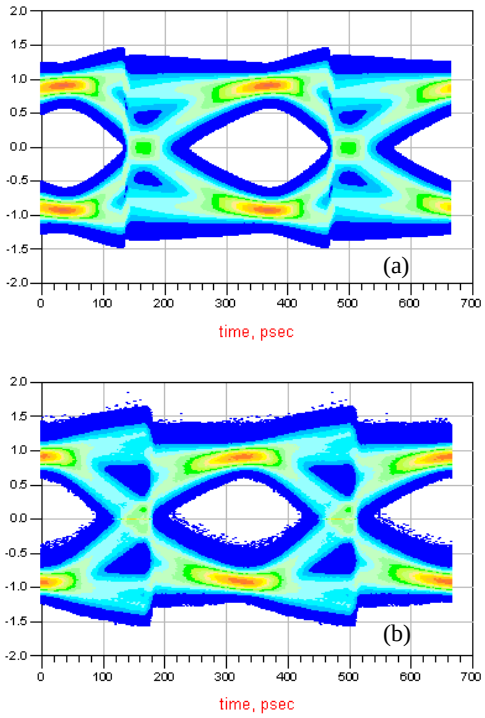


Figure 12: Eye diagrams with AMI models at 3 Gbps simulated by (a) the proposed statistical method, and (b) 1M bits time-domain simulation.

## VII. Conclusion

Statistical methods are widely adopted for high speed serial link simulation. Well established tools, such as StatEye, rely on approximate modeling of TX jitter and underestimate eye closure. More rigorous modeling requires new methods, able to cope with the computational complexity introduced by TX jitter. The paper reported on a highly efficient method that accommodates a rigorous treatment of TX jitter influence on channel performance. It captures effects that include RJ amplification by the channel, frequency dependent periodic jitter and asymmetric transitions due to DCD. The method has been validated by extensive numerical experiments and detailed comparisons with long Monte Carlo simulations.

## References

[1] B. Casper, M. Haycock, R. Mooney, "An accurate and efficient analysis method for multi-Gb/s chip-to-chip signaling schemes," *VLSI Circuit Symposium*, pp. 54-57, June 2002.

[2] A. Sanders, M. Resso, and J. D'Ambrosia, "Channel compliance testing utilizing novel statistical eye methodology," *DesignCon*, 2004.

[3] V. Stojanovic and M. Horowitz, "Modeling and analysis of high-speed links", *CICC 2003*, pp. 589-594, 2003.

[4] B. Casper, G. Balamurugan, J. Jaussi, J. Kennedy, M. Mansuri, F. O'Mahony, and R. Mooney, "Future microprocessor interfaces: analysis, design and optimization," *CICC 2007*, pp. 479-486.

[5] S. Chaudhuri, W. Anderson, J. McCall, and S. Dabrai, "Jitter amplification characterization of passive clock channels at 6.4 and 9.6 Gb/s," *Proc. IEEE 15th Topical Meeting on Electric Performance of Electronic Packaging*, Scottsdale, AZ, Oct. 2006, pp. 21-24.

[6] S. Chang, D. Oh and C. Madden, "Jitter Modeling in Statistical Link Simulation", *EMC'08*.

[7] IBIS Specifications 5.0.